Inorg. Chem. **2006**, *45*, 8408–8413

Neutron Diffraction Studies of U_4O_9: Comparison with EXAFS Results

F. Garrido

Centre de Spectrométrie Nucléaire et de Spectrométrie de Masse, CNRS-IN2P3, Université Paris-Sud, F-91405 Orsay Campus, France

A. C. Hannon and R. M. Ibberson

ISIS Facility, Rutherford Appleton Laboratory, Chilton, Didcot, Oxon OX11 0QX, U.K.

L. Nowicki

The Andrzej Soltan Institute for Nuclear Studies, ul. Hoza 69, PL-00-681 Warsaw, Poland

B. T. M. Willis*

Chemistry Research Laboratory, University of Oxford, Mansfield Road, Oxford OX1 3TA, U.K.

Received June 1, 2006

Conradson et al.[1] have analyzed X-ray absorption fine-structure spectra of the UO_2–U_4O_9 system and concluded that oxygen atoms are incorporated in U_4O_9 as oxo groups with U–O distances in the range 1.72–1.76 Å. They also found that the uranium sublattice consists of an ordered portion and an additional 'spectroscopically silent' glassy portion. We have carried out studies of powdered U_4O_9 by neutron diffraction which contradict these conclusions from EXAFS measurements. Our analysis shows that there are no U–O bonds shorter than 2.2 Å and that U_4O_9 is crystallographically ordered with no evidence of a glassy structure.

Introduction

At high temperatures, excess oxygen is incorporated in uranium dioxide, UO_2, to form UO_{2+x}, and as oxidation proceeds, many crystallographically distinct phases are formed in the range $0 < x < 1.0$. U_4O_9, with $x = 0.25$, is the first stoichiometric compound formed in this progressive oxidation. Conradson et al.[1] have carried out an extensive EXAFS study of the local structure and charge distribution in the $UO_2-U_4O_9$ system, making measurements at 80 K on samples with different values of x in the range 0−0.20. Although these samples were prepared at high temperature in the single-phase region of UO_{2+x}, they disproportionated at low temperatures into a mixture of UO_2 and U_4O_9.[2] For this reason, we shall assume that their new results relate to the phase U_4O_9 because there are no uncertainties regarding UO_2 which possesses the well-characterized cubic fluorite structure.[3]

These new results from EXAFS are of two kinds: (1) the additional oxygen atoms are incorporated as oxo groups with U−O distances in the range 1.72−1.76 Å; (2) the uranium sublattice contains a 'spectroscopically silent' glassy part. Here we describe neutron diffraction studies of powdered U_4O_9 with the aim of addressing the same questions: Does U_4O_9 possess U−O bonds which are shorter than 2.0 Å? Does U_4O_9 consist of both ordered and glass-like material?

The neutron diffraction data were collected using the High-Resolution Powder Diffractometer, HRPD, and the General Materials Diffractometer, GEM,[4] both located at the ISIS Facility of the Rutherford Appleton Laboratory. The neutron experiments led to conclusions which are at variance with those described by Conradson et al.[1]

* To whom correspondence should be addressed. E-mail: bertram.willis@chem.ox.ac.uk.

(1) Conradson, S. D.; Manara, D.; Wastin, F.; Clark, D. L.; Lander, G. H.; Marales, L. A.; Rebizant, J.; Rondinella, V. V. *Inorg. Chem.* **2004**, *43*, 6922. Conradson, S. D.; Begg, B. D.; Clark, D. L.; den Auwer, C.; Ding, M.; Dorhout, P. K.; Espinosa-Faller, F. J.; Gordon, P. L.; Haire, R. G.; Hess, N. J.; Hess, R. F.; Keogh, D. W.; Lander, G. H.; Manara, D.; Morales, L. A.; Neu, M. P.; Paviet-Hartmann, P.; Rebizant, J.; Rondinella, V. V.; Runde, W.; Tait, C. D.; Veirs, D. K.; Villella, P. M.; Wastin, F. *J. Solid State Chem.* **2005**, *178*, 521.

(2) Schaner, B. E. *J. Nucl. Mater.* **1960**, *2*, 110.

(3) Willis, B. T. M. *Proc. R. Soc. A* **1963**, *274*, 122.

(4) Hannon, A. C. *Nucl. Instrum. Methods A* **2005**, *551*, 88.

10.1021/ic060964c CCC: $33.50 © 2006 American Chemical Society
Published on Web 09/06/2006

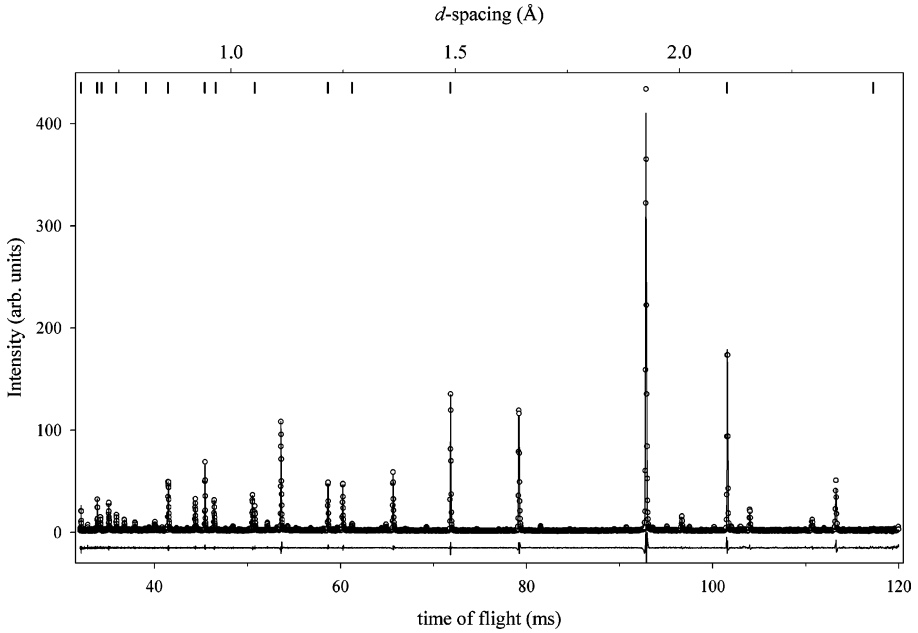

Figure 1. Multiphase time-of-flight powder pattern from HRPD of MgO and U_4O_9. The experimental data points are shown as circles, while the Rietveld refinement is shown as a line. The residual from the refinement is shown displaced below. Four of the vertical tick marks indicate the positions of the MgO reflections, and all other reflections are identifiable as arising from U_4O_9.

Experimental Procedure

Sample Preparation. The U_4O_9 powder was prepared by the method of oxygen transfer.[5−7] The principle of the method is the equilibration of the dissociation pressures of UO_2 and U_3O_8 heated together in a vacuum. Calculated amounts of stoichiometric UO_2 and U_3O_8 powders were placed in the two arms of an evacuated quartz glass tube. The UO_2 powder was annealed at 1400 °C in an Ar/H_2 (10%) reducing mixture in order to restore the stoichiometric composition. The starting U_3O_8 powder was heated at 500°C under air to decompose the uranium hydrates that can be formed during the storage period of the powder due to the presence of water in air and to provide the exact stoichiometry O/U = 2.667. The evacuated quartz tube was heated at a rate of 2 °C h^{-1} up to a temperature of 1100 °C, kept for one month at this temperature, then cooled at a rate of 2 °C h^{-1} down to room temperature. On the basis of the amounts of starting materials and on the equilibrium oxygen pressure at 1100 °C, the composition of the final U_4O_9 sample was expected to be 2.242 ± 0.001, which is within the homogeneity range for the U_4O_{9-y} phase.[7] The neutron diffraction pattern exhibited the characteristic features of the U_4O_9 phase, i.e., the presence of superlattice lines, due to small displacements of uranium atoms from the fluorite sites to form a cubic superstructure.[8,9]

HRPD Experiment. The U_4O_9 sample was mixed with an equal volume of crystalline magnesium oxide, MgO: the crystal structures of U_4O_9 and MgO are both known. The disordered fraction of U_4O_9 gives diffuse scattering but no Bragg peaks, and so the ratio of disordered to ordered U_4O_9 can be derived by measuring the Bragg intensities of the two components, U_4O_9 and MgO, and comparing this with the known weight ratio.

Table 1. GSAS Refinement of Powder Pattern

	weight fraction of U_4O_9	weight fraction of MgO
GSAS refinement	90.9 ± 0.5%	9.1 ± 0.5%
direct determination of weight	89.5%	10.5%

Figure 1 shows the intensity of a portion of the combined powder diffraction pattern as a function of time-of-flight. The flight times correspond to a relatively small range of Q ($=4\pi \sin\theta/\lambda$) given by

$$0.25\ \text{Å}^{-1} < Q < 0.85\ \text{Å}^{-1} \quad (1)$$

The pattern includes four Bragg peaks from MgO, which are indexed on a face-centered cubic cell of edge 4.22 Å. The remaining peaks are due to U_4O_9 and consist of strong *fundamental* lines, which are associated with the fluorite subcell of edge 5.44 Å, and weak *superlattice* lines arising from the assembly of 64 of these subcells in a cubic supercell of edge =21.76 Å. We note that the integral breadth of the diffraction peaks indicates that the crystallite size of the sample is not less than 7500 Å.

The powder pattern was analysed by the Rietveld procedure using the crystallographic program GSAS.[10] MgO has the rocksalt structure, and the only structural parameters to be varied in the program are the temperature factors of the Mg and O atoms. The variable parameters for U_4O_9 are the temperature factors of the U and O atoms and their atomic coordinates, *xyz*, whose starting values were given by the structural model of Cooper and Willis.[9] The refinement converged to give the weight fractions in the second row of Table 1. The third row in the table gives the weight fractions obtained by direct measurement.

The fractions derived from the Rietveld refinement are in approximate agreement with those obtained from direct weight

(5) Van Lierde, W.; de Jonghe L. *Solid State Commun.* **1964**, *2*, 129.
(6) Kotlar, A.; Gerdanian, P.; Dodé, M. *J. Chim. Phys.* **1967**, *64*, 862.
(7) Van Lierde, W.; Pelsmaekers, J.; Lecocq-Robert, A. *J. Nucl. Mater.* **1970**, *37*, 276.
(8) Bevan, D. J. M.; Grey, I. E.; Willis, B. T. M. *J. Solid State Chem.* **1986**, *61*, 1.
(9) Cooper, R. I.; Willis, B. T. M. *Acta Crystallogr. A* **2004**, *60*, 322.
(10) Larson, A. C.; von Dreele, R. B. *General Structure Analysis System GSAS*; Report MS-H805; Los Alamos National Laboratory: Los Alamos, NM, 2000.

measurements. There is no evidence of a glassy, disordered fraction at a level exceeding 1% or 2%.

Outline of Theory for Measurement of Neutron Correlation Functions. The quantity measured in a neutron diffraction experiment[11,12] is the differential cross-section

$$\frac{d\sigma}{d\Omega} = I^S(Q) + i(Q) \tag{2}$$

where $I^S(Q)$ is the self-scattering and $i(Q)$ is the distinct scattering. The self-scattering, which can be calculated approximately, is subtracted from the data to give the distinct scattering. Structural information may then be obtained by a Fourier transformation of $i(Q)$, yielding the differential correlation function

$$D(r) = \frac{2}{\pi}\int_0^\infty Qi(Q)M(Q)\sin(rQ)\,dQ \tag{3}$$

where $M(Q)$ is a modification function introduced to take into account the maximum experimentally attainable momentum transfer, Q_{max}, which leads to a broadening of the correlation function in real-space. The differential correlation function, $D(r)$, contains information relating to differences between the average density at a distance, r, from an average origin atom and the corresponding radial density for a homogeneous material. It is also useful to define the total correlation function as

$$T(r) = 4\pi r g^0 (\sum_l c_l \bar{b}_l)^2 + D(r) \tag{4}$$

where g^0 is the average atomic number density and the l summation is over elements. c_l and $\bar{b}_l$ are, respectively, the atomic fraction and coherent neutron scattering length for element l. A peak in $T(r)$ indicates an interatomic distance which occurs frequently in the sample, and its area is directly related to the coordination number for that distance.

Although the correlation function interpretation of diffraction data was developed for the study of non-crystalline materials, such as glasses and liquids, it has recently come to be applied to the study of crystalline materials, especially disordered crystals.[13] The extraction of the correlation function, $T(r)$, from experimental data does not involve any specific structural model. Thus, it provides a model-independent means of investigating the short- and medium-range order in a sample. For example, if a sample of U_4O_9 contains two portions, one of which is ordered on a regular crystalline lattice, while the other portion is glassy, then it might be expected that a conventional crystallographic technique (such as Rietveld refinement) would only be sensitive to the crystalline portion because such techniques only take into account the Bragg peaks and not the diffuse signal (if any) between the Bragg peaks. However, the total correlation function, $T(r)$, is inherently sensitive to all of the portions in the sample, since it involves integrations of the whole diffraction pattern, according to the Fourier transformation of eq 3. That is to say, when using a correlation function analysis, it is impossible for there to be a "spectroscopically silent" portion of the sample.

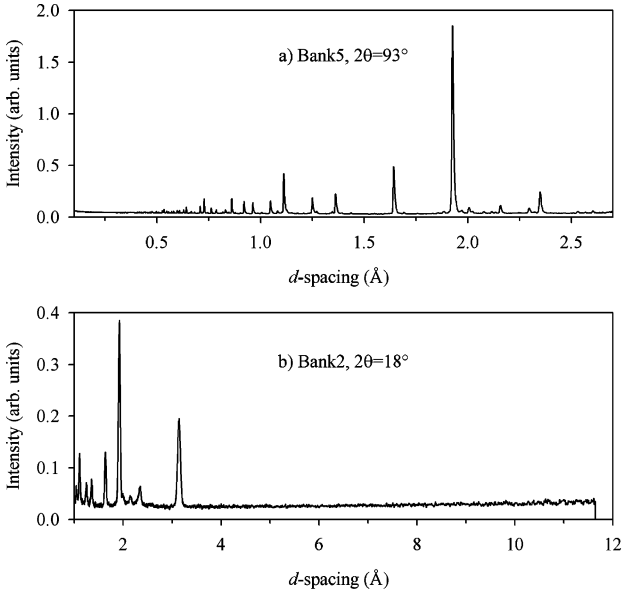

Figure 2. Intensity versus d-spacing for (a) Bank5 and (b) Bank2 on GEM. (In (b), the two strongest lines are fundamental peaks and the rest are superlattice peaks.)

The GEM Experiment. For the GEM[4] experiment, a 2.2 g sample of U_4O_9 (without MgO) was sealed inside a drawn vanadium container of internal and external radius 0.2985 and 0.3175 cm, respectively. Neutron diffraction data were recorded with the sample at ambient temperature (i.e., approximately 25 °C). The data were normalized relative to the scattering from a vanadium rod of diameter 0.834 cm. Figure 2 shows the powder diffraction pattern measured in two of the eight detector banks of GEM. Weak superlattice reflections are clearly seen in the low-angle bank, but the overall background is smooth and gives no indication of diffuse scattering from an amorphous phase. The experimental data used for the correlation function analysis, in both reciprocal- and real-space, are available from the ISIS Disordered Materials Database.[14]

A full set of experimental corrections was performed using the gudrun program[15] and the ATLAS suite of software.[12] The self-scattering was calculated using the Placzek approximation,[16] implemented for time-of-flight diffraction.[17] Figure 3 shows the corrected distinct scattering, $i(Q)$, obtained by a combination of data from detector banks 1, 2, 3, 4, and 5 (at mean scattering angles of 9°, 18°, 35°, 62°, and 93°) on the GEM diffractometer.[4] There is no diffuse contribution to the distinct scattering, such as would be observed for a "spectroscopically silent" glassy portion of the sample. Figure 4 shows the differential correlation function, $D(r)$, obtained by a Fourier transformation of the distinct scattering, according to eq 3, using the Lorch modification function[18] with a Q_{max} of 45 Å^{-1}. The linear term plotted at low r is calculated from the negative of the first term on the right-hand side of eq 4. This term is determined by the density and composition of the sample; its agreement with the experimental $D(r)$ in this region indicates

(11) Wright, A. C. *Adv. Struct. Res. Diffr. Methods* **1974**, *5*, 1. Hannon, A. C. In *Encyclopedia of Spectroscopy and Spectrometry*; Lindon, J., Tranter, G., Holmes, J., Eds.; Academic Press: London, 2000; Vol. 2, p 1493. Hannon, A. C. In *Encyclopedia of Spectroscopy and Spectrometry*; Lindon, J., Tranter, G., Holmes, J., Eds.; Academic Press: London, 2000; Vol. 2, p 1479.
(12) Hannon, A. C.; Howells, W. S.; Soper, A. K. *IOP Conf. Ser.* **1990**, *107*, 193.
(13) Egami, T. In *Local Structure from Diffraction*; Billinge, S. J. L., Thorpe, M. F., Eds.; Plenum Press: New York, 1998; p 1. Hibble, S. J.; Hannon, A. C. In *From semiconductors to proteins: beyond the average structure*; Billinge, S. J. L., Thorpe, M. F., Eds.; Kluwer Academic/Plenum Publishers: New York, 2002; p 129. Billinge, S. J. L.; Kanatzidis, M. G. *Chem. Comm.* **2004**, 749.
(14) Hannon A. C. **2001**, *ISIS Disordered Materials Database*, http://www.isis.rl.ac.uk/disordered/Database.
(15) Soper, A. K.; Buchanan, P. Private communication, 2004.
(16) Placzek, G. *Phys. Rev.* **1952**, *86*, 377.
(17) Howe, M. A.; McGreevy, R. L.; Howells, W. S. *J. Phys.: Condens. Matter* **1989**, *1*, 3433.
(18) Lorch, E. *J. Phys. C* **1969**, *2*, 229.

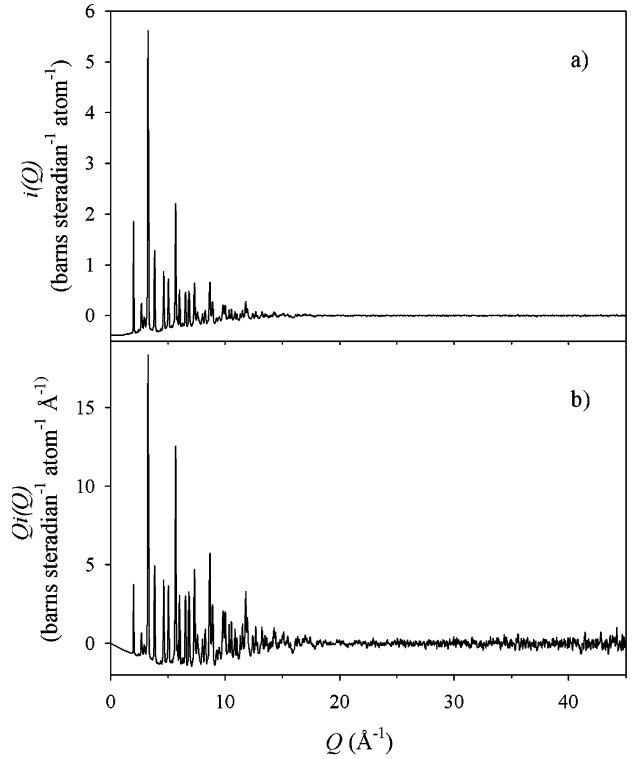

Figure 3. Total diffraction data for U_4O_9 measured on GEM, showing (a) the distinct scattering, $i(Q)$, and (b) the interference function, $Qi(Q)$.

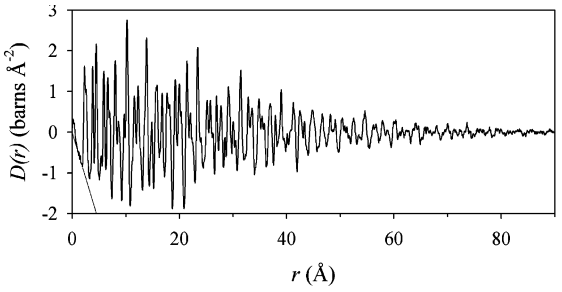

Figure 4. Differential correlation function, $D(r)$, for U_4O_9 measured on GEM. The linear function shown at low r is calculated from the negative of the first term on the right-hand side of eq 4.

that the data are correctly normalized, which is crucial for a satisfactory calculation of the total correlation function, $T(r)$, and the extraction of coordination number information. (The quality of the diffraction data can be judged from the behavior of $D(r)$ and $T(r)$ at low values of r.) Structural oscillations are readily apparent in the correlation function for interatomic distances up to and beyond about 70 Å, indicating a high degree of ordered crystallinity in the material. The absence of the oscillations beyond this distance is not due to a finite domain or crystallite size but is rather due to a progressive damping which arises from the instrumental resolution in reciprocal (i.e., Q-) space.[19]

Comparison with EXAFS

Figure 5 shows the experimental total correlation function, $T_{exp}(r)$, derived by adding the average density contribution to the differential correlation function, $D(r)$, according to eq 4. The non-zero region of $T(r)$ below about 0.7 Å (and also the oscillations at about 1.3 and 1.6 Å) does not represent real physical interatomic distances, but instead the feature in this region is an error peak which arises from imperfections in the experimental corrections for experimental effects, such as absorption, multiple scattering, and inelasticity.[18] The error peaks are relatively large for this measurement due to the small sample size and the need for thick sample containment of a uranium oxide sample. The positions of the first real peaks, due to U−O and O−O correlations, are indicated in Figure 5 by vertical arrows at distances of 2.33 and 2.66 Å, respectively.

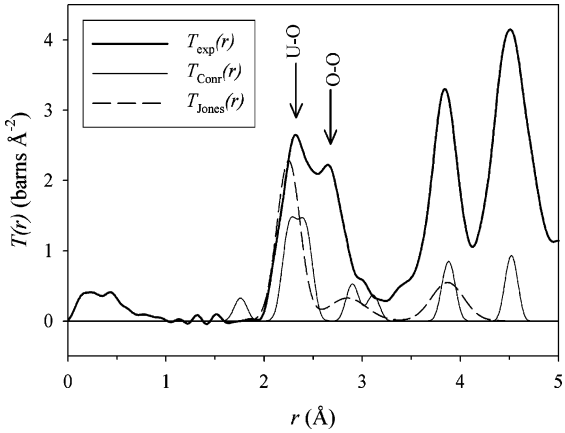

Figure 5. Total correlation function, $T_{exp}(r)$, for U_4O_9 measured on GEM (thick line), with the positions of the first U−O and O−O peaks indicated by vertical arrows. Also shown are simulations of the total correlation function calculated using the EXAFS parameters for $UO_{2.20}$[1] (thin line) and for U_4O_9[21] (dashed line).

Conradson et al.[1] have used uranium L-III edge EXAFS to study a series of UO_{2+x} samples at a temperature of about 80 K, determining the interatomic distance, coordination number, and Debye−Waller factor (R, N, and σ) for a number of shells for each sample. The EXAFS results for the most oxygen-rich composition studied, $UO_{2.20}$, are reproduced in Table 2. We used these parameters to calculate a simulation of the neutron correlation function, $T_{Conr}(r)$, and this is shown in Figure 5 together with the experimental function, $T_{exp}(r)$, measured on GEM. The simulation was calculated using the formalism for the contribution to $T(r)$ due to a single interatomic distance given by Hannon et al.,[20] and it was assumed that the "Debye−Waller factor", σ, given by Conradson et al.[1] is equal to the root-mean-square variation in interatomic distance between atoms of type j and k, $<u^2_{j-k}>^{1/2}$.

EXAFS is an element-specific technique, and uranium edge results are sensitive to U−O and U−U correlations, but not to O−O correlations. Thus, the simulated function, $T_{Conr}(r)$, should not be expected to reproduce the first O−O peak at 2.66 Å. Also, EXAFS is not sensitive to longer distances, and hence the simulated function should not be expected to agree with the neutron diffraction result for larger values of r. The EXAFS results should, however, be able to predict the measured neutron correlation function for distances in the range below about 2.6 Å, where only U−O

(19) Grimley, D. I.; Wright, A. C.; Sinclair, R. N. *J. Non-Cryst. Solids* **1990**, *119*, 49.

(20) Hannon, A. C.; Grimley, D. I.; Hulme, R. A.; Wright, A. C.; Sinclair, R. N. *J. Non-Cryst. Solids* **1994**, *177*, 299.

Table 2. EXAFS Results for $UO_{2.20}$[1] and U_4O_9[21]

Conradson et al.[1]				Jones et al.[21]			
assignment	R (Å)	N	σ (Å)	assignment	R (Å)	N	σ (Å)
U−O	1.76(1)	0.3(1)	0.045(7)				
U−O	2.26(2)	1.8(5)	0.057(13)	U−O	2.25(2)	5(1)	0.11(3)
U−O	2.42(2)	1.9(6)	0.057(13)				
U−O	2.90(1)	0.8(2)	0.045(9)	U−O	2.85(7)	1.5(6)	0.19(5)
U−O	3.11(1)	0.6(1)	0.045(6)				
U−U	3.880(9)	2.5(6)	0.050(7)	U−U	3.87(24)	4(2)	0.16(2)
U−O	4.52(1)	2.2(7)	0.045(13)				

correlations are expected. In practice, as Figure 5 shows, there is poor agreement in this range between the EXAFS-derived simulation and the correlation function measured by neutron diffraction. First, there is no evidence from neutron diffraction for a short U−O distance close to 1.76 Å, which Conradson et al.[1] have interpreted as evidence for oxo groups in $UO_{2.20}$, associated with U^{6+}. Second, the EXAFS results underestimate the area under the correlation function for distances below 2.6 Å by a factor of order two. That is to say, the EXAFS results significantly underestimate the U−O coordination number.

Figure 5 also shows a calculation of the correlation function, $T_{\text{Jones}}(r)$, based on the parameters from an earlier EXAFS study of U_4O_9 (see Table 2).[21] It is notable that these results do not include a U−O oxo bond in the range 1.72−1.76 Å and that they lead to a correlation function which is closer to the correlation function, $T_{\text{exp}}(r)$, determined by neutron diffraction in the region of the first U−O peak.

Comparison with Rietveld Analysis

Figure 6 shows a comparison between the total correlation function, $T_{\text{exp}}(r)$, measured on GEM and a simulation of the correlation function derived from the crystal structure data[22] for U_4O_9. The XTAL program[23] was used to calculate the partial radial distribution functions from the lattice parameters and atomic coordinates determined from Rietveld analysis of neutron powder diffraction data.[22] These were then broadened for the effects of thermal motion and real-space resolution (arising from the modification function, $M(Q)$, as in eq 3), and were scaled according to the U_4O_9 atomic fractions and neutron scattering lengths of uranium and oxygen. In this process, the root-mean-square variation in interatomic distance, $<u^2_{j-k}>^{1/2}$, for each pair of atoms was chosen to optimize the agreement with the experimental correlation function, as follows. $<u^2_{\text{U-U}}>^{1/2} = <u^2_{\text{O-O}}>^{1/2} = 0.1$ Å, $<u^2_{\text{U-O}}>^{1/2} = 0.13$ Å.

The simulated contributions to the total correlation function involving uranium, U−U and U−O, give a good agreement with the measured total correlation function, while the simulated O−O contribution agrees less well. The first O−O peak has a reasonable area, but it is at too short a distance, with an error of order 0.1 Å, and the distribution of O−O distances is too broad. The comparison shown in Figure 6 is to be contrasted with the comparison with EXAFS results shown in Figure 5, which shows that EXAFS results are not at all consistent with the measured correlation function of U_4O_9. The results from Rietveld analysis are mostly consistent with the measured correlation function, but nevertheless, the comparison suggests that there is scope for improvement in the Rietveld model.

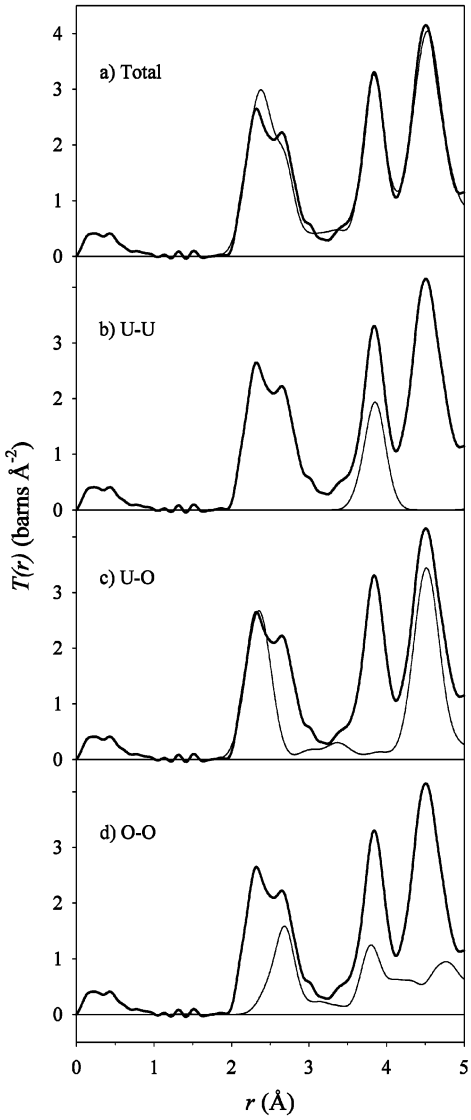

Figure 6. Total correlation function, $T_{\text{exp}}(r)$, for U_4O_9 measured on GEM (thick line), together with the following simulated contributions to the correlation function (thin lines), calculated from the structural parameters of U_4O_9 derived from Rietveld refinement of neutron powder diffraction data: (a) the total correlation function, (b) the U−U contribution, (c) the U−O contribution, and (d) the O−O contribution.

(21) Jones, D. J.; Roziere, J.; Allen, G. C.; Tempest, P. A. *J. Chem. Phys.* **1986**, *84*, 6075.
(22) Garrido, F.; Ibberson, R. M.; Nowicki, L.; Willis, B. T. M. In preparation.
(23) Hannon, A. C. Rutherford Appleton Laboratory Report RAL-93-063, 1993.

UO_2 has the calcium fluorite structure, in which the oxygens are arranged on a cubic lattice, and then the uraniums are positioned at the center of every alternate oxygen cube. Each uranium has eight oxygen neighbors at a distance 2.368 Å, and the oxygens are separated by 2.734 Å. The structure of U_4O_9 is a modification of the UO_2 structure, where the extra oxygens are incorporated by a rearrangement of the oxygens around the center of a vacant cube, which has been described[8,9] as having the geometry of a cuboctahedron. The current results suggest the need for a modification of this geometry so that there is a small increase in the oxygen−oxygen separation. However, it should be emphasized that, despite this small discrepancy, there is no evidence from this comparison for a fundamental re-evaluation of the view of the structure of U_4O_9 as being a conventional crystalline compound. We have found no evidence for short oxo U−O bonds, we have found no evidence for a "spectroscopically silent glassy part" of the structure, and we have found no evidence for coordination numbers significantly at variance with those predicted by the crystal structure determined from diffraction studies.

A possible explanation for the discrepancy between the neutron diffraction and EXAFS coordination numbers is suggested by a consideration of the thermal factors. We have found that a value of 0.13 Å is required for the root-mean-square variation in U−O distances, $<u^2_{U-O}>^{1/2}$, to obtain reasonable agreement between the measured correlation function, $T_{exp}(r)$, and the correlation function, $T_{U-O}(r)$, simulated from the crystal structure results. However, on the basis of EXAFS studies, Conradson et al.[1] have reported values for σ ($=<u^2_{U-O}>^{1/2}$) which are less than half our value (see Table 2). It is well known that, in fitting EXAFS spectra, the coordination number, N, and the Debye−Waller factor, σ^2, are strongly correlated.[24] For example, if σ^2 is constrained to have too small a value in fitting EXAFS data, then this results in N also being too small. It is therefore to be expected that an unreasonably small coordination number is associated with a thermal factor which is also too small. Support for this suggestion may be found from other uranium L-III edge EXAFS studies, in which a value for σ in the region of 0.1 Å is generally found for U−O distances longer than 2.0 Å,[25] irrespective of whether uranium has a valence of 4+, 5+, or 6+. Furthermore, it may be noted that the earlier EXAFS study of U_4O_9[21] had σ values (see Table 2) which are larger than those reported by Conradson et al.[1], and which are broadly consistent with the $<u^2_{j-k}>^{1/2}$ values that we have found to be required in order to obtain reasonable agreement between the measured correlation function, $T_{exp}(r)$, and the correlation function, $T_{U-O}(r)$, simulated from the crystal structure results. This earlier study also gives coordination number information which is closer in agreement to what we have determined by neutron diffraction, as is demonstrated by the comparison shown in Figure 5.

(24) Gurman, S. J. *J. Synchrotron Rad.* **1995**, *2*, 56.

(25) Barrett, N. T.; Greaves, G. N.; Willis, B. T. M.; Antonini, G. M.; Thornley, F. R. *J. Phys. C* **1988**, *21*, L791. Fortner, J. A.; Kropf, A. J.; Finch, R. J.; Bakel, A. J.; Hash, M. C.; Chamberlain, D. B. *J. Nucl. Mater.* **2002**, *304*, 56. O'Loughlin, E. J.; Kelly, S. D.; Cook, R. E.; Csencsits, R.; Kemner, K. M. *Environ. Sci. Technol.* **2003**, *37*, 721. Denecke, M. A.; Janssens, K.; Proost, K.; Rothe, J.; Noseck, U. *Environ. Sci. Technol.* **2005**, *39*, 2049. Hennig, C.; Tutschku, J.; Rossberg, A.; Bernhard, G.; Scheinost, A. C. *Inorg. Chem.* **2005**, *44*, 6655.

Conclusions

We conclude that the results obtained on the U_4O_9 system are quite different according to whether the analysis is performed on EXAFS data or on diffraction data. However, we must acknowledge that the two studies were carried out on samples of different chemical composition. The EXAFS study was carried out on samples of UO_{2+x} (with $0.00 < x < 0.20$) at liquid-nitrogen temperature, and if the samples were in thermodynamic equilibrium at this temperature, they consisted of a mixture of UO_2 and U_4O_9. Table 2 of Conradson et al., therefore, gives interatomic spacings for UO_2 (with the cubic fluorite structure) together with the spacings for U_4O_9: the spacings for UO_2 are well known and can be readily identified in this table. Even after allowance has been made in the EXAFS analysis for the presence of UO_2, it would appear that the conclusions from the two techniques are irreconcilable. If U_4O_9 consists of both a glassy and an ordered phase, the diffraction data indicate that the proportion of the glassy phase cannot exceed 2%.

The term UO_{2+x} is used by Conradson et al.[1] in the title and text of their papers. This term is used widely to denote a single phase consisting of a solid solution of UO_2 and oxygen. In fact, all the samples for the EXAFS study were various mixtures of the two distinct phases, UO_2 and U_4O_9, produced by cooling UO_{2+x} to room temperature. They were not the single phase UO_{2+x} (Schaner[2] has described extensive electron-microscopic and metallographic analyses of such samples.) A proper EXAFS investigation would require the examination of either the phase UO_{2+x} at high temperature or the phase U_4O_9 at ambient temperature.

IC060964C